

Dynamical electric dipole theory for quantitatively describing coupled split-ring resonators

Yong Zeng and Douglas H. Werner

Department of Electrical Engineering, Pennsylvania State University, University Park, Pennsylvania 16802

Compiled November 20, 2018

Metallic split-ring resonators possess dominant electric dipoles as well as considerable magnetic dipoles under proper excitations. Full-wave numerical approaches are frequently employed to simulate adjacent split-ring resonators, but simulations cannot explain the underlying physics. An analytical theory based on a dynamic electric dipole approximation is developed here. Detailed theory-simulation comparisons demonstrate that this theory can *quantitatively* describe the interaction strength of coupled split-ring-resonators under certain circumstances. © 2018 Optical Society of America

OCIS codes: 220.1080, 240.6680, 350.4990

Since its introduction in 1999, metallic split-ring resonators (SRRs) have attracted intense attention because of their important roles in artificial metamaterials [1]. Under appropriate illumination, circulating current will be excited inside the SRR and lead to magnetic dipoles comparable in magnitude to electric dipoles, making metallic SRRs ideal building blocks to achieve strong magnetic responses in the optical region. A single SRR consequently is referred to as a magnetic photonic atom [2]. Recently, several experiments are devoted to multipole coupling between SRRs, especially electric and magnetic dipole interaction [3–6]. For instance, planar metallic SRR arrays are fabricated with different lattice spacing along different directions, and both magnetic and electric near-field dipole coupling are found to simultaneously influence the spectral positions of the plasmonic resonances [5]. Another experiment studied isolated metallic SRR dimers with different configurations. Changing the relative magnetic dipole phase of the constituent particles identifies the strength of magnetic dipole coupling [4]. Two methods are frequently employed to interpret the experimental observations, full-wave numerical simulations and quasistatic coupling models. Simulations are able to reproduce the experimental measurements quantitatively, but shed little light on the underlying physics [4]. The quasistatic model, on the other hand, obtains variables by fitting experimental data. Consequently it can not make an *a priori* prediction [5–7].

In this Letter we will show that *a priori* predictions of the electromagnetic interaction are feasible for specific SRRs structures. More particularly, we carefully compare the dynamic radiation emitted from the magnetic dipole of a single SRR with that from its electric counterpart. It is found that at particular “safe” spatial regions the electric dipole exclusively dominates the radiation field. An individual SRR consequently can be approximated by an isotropic electric dipole whose polarizability is determined by the particle geometry as well as the illumination. This approximation can be further extended

to multiple SRRs where each constituent particle sits in the safe zone of other particles. Two dimers are studied to verify our theory. By comparing the analytical results with the corresponding full-wave numerical results, it is demonstrated that our theory allow us to predict the coupling strength *quantitatively*.

We start with the optical response of a gold SRR as shown in Fig. 1(a), which closely matches the experimental samples of Ref. [5]. It is excited by an x -polarized plane wave propagating in the z direction. The absolute extinction and absorption cross section of the particle are shown in Fig. 1(b) [8]. A peak corresponding to the fundamental plasmonic resonance was found at a wavelength of 1352 nm. Because of the structural symmetry breaking, a z -component magnetic dipole m_z is generated together with a dominant x -component electric dipole d_x . Numerical simulations further suggest that the ratio $\beta = -m_z/d_x/c$ is around 0.29i [8]. The magnetic dipole therefore has an amplitude comparable to its electric counterpart. In addition, because the extinction spectra are very sensitive to the illumination polarization, both electric and magnetic dipoles are strongly anisotropic [5, 8].

It is well known that the electric field, in the near and far zone, for an electric dipole source \mathbf{p} is given by [9]

$$\mathbf{E}_e(\mathbf{r}) = [A(kr)\mathbf{I} + B(kr)\mathbf{T}] \cdot \mathbf{p} \quad (1)$$

with k being the wave number, \mathbf{I} being an unit tensor of rank 2. The tensor \mathbf{T} has component as $T_{ij} = r_i r_j / r^2$, and the coefficients are written as [10]

$$\begin{aligned} A(kr) &= \frac{e^{ikr}}{4\pi\epsilon_0 r^3} (k^2 r^2 + ikr - 1), \\ B(kr) &= \frac{e^{ikr}}{4\pi\epsilon_0 r^3} (3 - 3ikr - k^2 r^2). \end{aligned} \quad (2)$$

The electric fields emitted from the electric dipole d_x of a single SRR are therefore direction-dependent: The A term survives for any radiation direction while the B term vanishes when \mathbf{r} parallels the y axis. In a similar way, the radiation for a magnetic dipole source \mathbf{m} bears

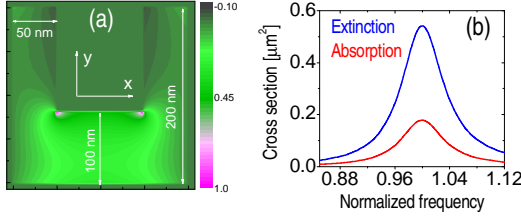


Fig. 1. (a) The x -component of the current distribution of an individual split-ring resonator at its fundamental resonance. The incident pulse is x -polarized and propagating in the z direction. (b) The extinction and absorption cross sections of the single split-ring resonator. The frequency is normalized to the fundamental resonant frequency ω_0 . The bulk plasma frequency of gold is taken as $\omega_p = 1.367 \times 10^{16} \text{s}^{-1}$, the phenomenological collision frequency $\gamma = 6.478 \times 10^{13} \text{s}^{-1}$.

the form

$$\mathbf{E}_m(\mathbf{r}) = -\frac{Z_0 k^2}{4\pi r^2} e^{ikr} (\mathbf{r} \times \mathbf{m}) \left(1 + \frac{i}{kr}\right). \quad (3)$$

with $Z_0 = \sqrt{\mu_0/\epsilon_0}$ being the vacuum impedance. The polarization of the radiation field therefore is perpendicular to the plane defined by \mathbf{r} and \mathbf{m} . Consequently, the electric field emitted from the magnetic dipole m_z is polarized in the xy plane and is perpendicular to \mathbf{r} when \mathbf{r} lies in the xy plane.

We now can analyze the radiation field of the single SRR in the xy plane. Because its fundamental wavelength, 1352 nm, is much larger than its characteristic size, higher-order multipoles fall off rapidly and the radiation emitted from the structure will come mainly from its electric and magnetic dipoles when $kr > 1$ [9]. More specifically, when \mathbf{r} parallels \mathbf{e}_x , \mathbf{E}_e is x -polarized and \mathbf{E}_m is y -polarized, and the ratio of their amplitude E_e/E_m equals $2/|\beta|kr$. The magnetic dipole then dominates the radiation zone where $kr \gg 1$, and the electric dipole dominates a limited region where $1 < kr < 1/|\beta|$. Similarly, the polarization of both \mathbf{E}_e and \mathbf{E}_m are along the x axis for \mathbf{r} parallel to \mathbf{e}_y . The amplitude ratio E_e/E_t , with \mathbf{E}_t being $\mathbf{E}_e + \mathbf{E}_m$, is further given by $[kr + i(1 - k^2 r^2)] / [kr + |\beta| + i(1 - k^2 r^2)]$. As a result, we can safely neglect the magnetic dipole and use the dynamic electric dipole approximation when $kr \gg |\beta|$. Similar conclusions apply for \mathbf{r} along the z axis. The electric vector \mathbf{E}_m is exactly zero because \mathbf{r} parallels m_z , and the \mathbf{E}_e is x -polarized. For a considerably large kr , the magnetic dipole has no influence on the radiation field.

The discussions above can be extended to multiple SRRs, as long as each constituent particle sits in the public “safe” zone. To validate the theory, we investigate two different configurations of SRR dimers, side-by-side

and on-top, which have been studied experimentally [4]. The dipole polarizability $\alpha(\omega)$ of an individual SRR is determined first, which connects to the extinction cross-section spectrum $\sigma(\omega)$ as [8]

$$\frac{Z_0}{|E_0|^2} \text{Re} \left[\mathbf{E}_0^* \cdot \int_v \mathbf{J}(\mathbf{r}') e^{-i\mathbf{k}_0 \cdot \mathbf{r}'} d\mathbf{r}' \right] \approx Z_0 \omega \text{Im} [\alpha(\omega)], \quad (4)$$

where \mathbf{E}_0 stands for the incident electric field, \mathbf{J} represents the polarization current and the integration is performed over the particle volume. We neglect the retarded effect because the particle height, 25 nm, is much shorter than the incident wavelength. Moreover, a Lorentz model describes the polarizability $\alpha(\omega)$ around the resonance

$$\alpha(\omega) = \frac{4\pi\epsilon_0 f}{\omega_0^2 - \omega^2 - i\omega\tau}, \quad (5)$$

where ω_0 is the resonant frequency, f stands for the oscillator strength and τ measures the phenomenological damping force [9]. For the SRR shown in Fig. 1(a), we find that $\tau/\omega_0 \approx 0.072$ as well as $f/\tau \approx 1.29 \times 10^{-5}$. It should be emphasized that the extinction spectrum is experimentally measurable [4, 11] and the parameters of the Lorentz model can then be obtained by fitting the experimental results.

By approximating each particle of an SRR dimer as an electric dipole, a set of coupled equations describes its optical properties

$$\mathbf{p}_1 = \alpha(\omega) [\mathbf{E}_0 + \mathbf{E}_e(\mathbf{d}, \mathbf{p}_2)], \quad \mathbf{p}_2 = \alpha(\omega) [\mathbf{E}_0 + \mathbf{E}_e(\mathbf{d}, \mathbf{p}_1)], \quad (6)$$

where \mathbf{d} stands for the distance between \mathbf{p}_1 and \mathbf{p}_2 , with \mathbf{p}_1 and \mathbf{p}_2 being the dipole moment of each particle, respectively. The symmetry of the equations immediately implies that the incident plane wave \mathbf{E}_0 only excites the symmetrical (in-phase) mode in either configuration. The extinction spectrum can be obtained by solving the set of equations. For the side-by-side structure it is given by

$$\sigma_e(\omega, d) = \text{Im} \left[\frac{2Z_0\omega}{\alpha(\omega)^{-1} - A(kd) - B(kd)} \right], \quad (7)$$

and for the on-top arrangement it is

$$\sigma_e(\omega, d) = \text{Im} \left[\frac{2Z_0\omega}{\alpha(\omega)^{-1} - A(kd)} \right]. \quad (8)$$

Because A and $A+B$ tend to zero when d goes to infinity, the equations above lead to an intuitive fact: The total power taken from the incident wave by two identical particles without coupling is twice of that by a single particle. Furthermore, the resonant frequency ω_r corresponds to the vanishing of the real part of the denominator of σ_e [10], we therefore have

$$4\pi\epsilon_0 \text{Re}[A(\omega_r d/c)] = \frac{\omega_0^2 - \omega_r^2}{f}, \quad (9)$$

for the on-top configuration, and

$$4\pi\epsilon_0 \text{Re}[A(\omega_r d/c) + B(\omega_r d/c)] = \frac{\omega_0^2 - \omega_r^2}{f}, \quad (10)$$

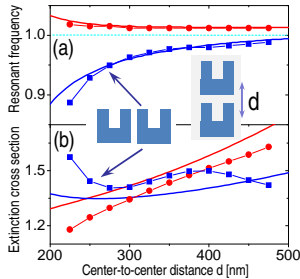


Fig. 2. Two different configurations, side-by-side and on-top, of two split-ring resonators. The resonant frequencies are normalized to ω_0 , the fundamental resonant frequency of the individual split-ring resonator. The extinction cross sections are normalized to the $\sigma_s(\omega_0)$, the extinction cross section of the single split-ring resonator at its fundamental resonance. The analytical and numerical results are shown with solid and dotted curves, respectively.

for the side-by-side configuration. Notice that the damping force τ of the Lorentz model does not appear since it mainly influences the bandwidth of the resonance [9]. These equations can be solved easily in the near-field zone where $kr \ll 1$. We find that $4\pi\epsilon_0\text{Re}[A] \approx -1/d^3$ as well as $4\pi\epsilon_0\text{Re}[A+B] \approx 2/d^3$, the resultant ω_r is therefore bigger than ω_0 for the on-top dimer while smaller than ω_0 for the side-by-side arrangement. In addition, the resonance shift $|\omega_r - \omega_0|$ of the side-by-side structure is considerably bigger than that of the on-top configuration [12]. The former structure therefore dominates the nearest neighbor coupling of equally oriented SRRs in dense square arrays [5]. We want to stress that all the predictions here are qualitatively consistent with the experimental observations [4, 5].

Equations (9) and (10) are solved for the separation d ranging from 200 to 500 nm, and the results are plotted in Fig. 2(a) with solid curves. The resonant frequencies ω_r are normalized to ω_0 of the individual particle. A finite-difference time-domain method is then applied to numerically simulate the two dimers, and the calculated results are plotted in Fig. 2(a) with dotted curves [13]. The center-to-center distance d , as marked in Fig. 2, is gradually increased from 225 nm to 475 nm (corresponding to kd from 1.0 to 2.2) with an increment of 25 nm. Notice that the width of the gap between these two particles is given by $d - 200$ nm; they are very close to each other. The numerical result of the on-top dimer is found to agree perfectly with its analytical counterpart when $d \geq 250$ nm, while a slight discrepancy appears for the side-by-side configuration: The numerical result oscillates around its analytical counterpart with an average relative difference smaller than 1%. It is possibly induced by the non-uniform distribution of the polarization current inside the SRR. As shown in Fig. 1(a), the

current is found to be strongly localized around the two inner corners. Assuming the current “hot” points are the positions of the electric dipoles, the dipole-to-dipole distance is shortened to roughly $d - 100$ nm for the side-by-side dimer. Higher-order multipoles such as an electric quadrupole may interfere with the electric dipole to a certain degree.

Although our theory describes the coupling strength *quantitatively*, it can not be extended to the extinction, absorption or scattering spectra because these quantities need the information regarding radiation along all the directions. However, its predictions can serve as a first approximation since the dominant electric dipole is contained. Take the two SRR dimers studied above as examples: their normalized extinction cross sections versus d are computed analytically and numerically, and the results are plotted in Fig. 2(b). Unlike the resonant frequency, the analytical results of the extinction are considerably different from their numerical counterparts, with an average relative difference around 10%. In addition, the theory must be employed cautiously to study the gap-to-gap and back-to-back configurations considered in Ref. [4]. The constituent particle in either dimer has in-phase electric dipoles but out-of-phase magnetic dipoles; Equation (6) then loses its validity. It is still a good approximation when d is big enough because the magnetic dipole coupling falls off rapidly with increasing inter-particle spacing. Finally, note that magnetoinductive coupling will appear in the side-by-side dimer when $d \gg c/|\beta|\omega_0$, as suggested by our theory [2].

To summarize, by carefully analyzing the fields emitted from the electric dipole and magnetic dipole of an individual split-ring resonator, we demonstrate that in certain circumstances a simple dynamic electric dipole can be employed to approximate the split-ring resonator. Two configurations of coupled split-ring resonators are studied to validate our theory by detailed theory-simulation comparisons. It is shown that this theory can predict coupling strength quantitatively and other optical quantities such as extinction cross section qualitatively.

We thank Lujun Huang for assistants. This work was supported in part by the Penn State Materials Research Science and Engineering Center under National Science Foundation (NSF) grant no. DMR 0213623.

References

1. J. B. Pendry, A. J. Holden, D. J. Robbins, and W. J. Stewart, IEEE Trans. Microwave Theory Tech. 47, 2075 (1999); D. R. Smith, W. J. Padilla, D. C. Vier, S. C. Nemat-Nasser, and S. Schultz, Phys. Rev. Lett. 84, 4184 (2000); S. Linden, C. Enkrich, M. Wegener, J. Zhou, T. Koschny, and C. M. Soukoulis, Science 306, 1351 (2004); R. Merlin, Proc. Natl. Acad. Sci. U.S.A. 106, 1693 (2009); M. Decker, S. Linden, and M. Wegener, Opt. Lett. 34, 1579 (2009); A. E. Nikolaenko, F. De Angelis, S. A. Boden, N. Papisimakis, P. Ashburn, E. Di Fabrizio, and N. I. Zheludev, Phys. Rev. Lett. 104,

- 153902 (2010).
2. L. Solymar and E. Shamonina, *Waves in Metamaterials* (Oxford University, 2009).
 3. F. Hesmer, E. Tatartschuk, O. Zhuromskyy, A. A. Radkovskaya, M. Shamonin, T. Hao, C. J. Stevens, G. Faulkner, D. J. Edwards, and E. Shamonina, *Phys. Status Solidi B* 244, 1170 (2007); N. Liu, S. Kaiser, and H. Giessen, *Adv. Mater.* 20, 4521 (2008); M. Decker, S. Burger, S. Linden, and M. Wegener, *Phys. Rev. B* 80, 193102 (2009).
 4. N. Feth, M. König, M. Husnik, K. Stannigel, J. Niegemann, K. Busch, M. Wegener, and S. Linden, *Opt. Express* 18, 6545 (2010).
 5. I. Sersic, M. Frimmer, E. Verhagen, and A. F. Koenderink, *Phys. Rev. Lett.* 103, 213902 (2009).
 6. N. Liu, H. Liu, S. Zhu, and H. Giessen, *Nat. Photonics* 3, 157 (2009).
 7. W. Rechberger, A. Hohenau, A. Leitner, J. R. Krenn, B. Lamprecht, and F. R. Aussenegg, *Opt. Commun.* 220, 137 (2003); H. Liu, D. A. Genov, D. M. Wu, Y. M. Liu, J. M. Steele, C. Sun, S. N. Zhu, and X. Zhang, *Phys. Rev. Lett.* 97, 243902 (2006).
 8. Y. Zeng, C. Dineen, and J. V. Moloney, *Phys. Rev. B* 81, 075116 (2010).
 9. J. D. Jackson, *Classical Electrodynamics*, 3rd ed. (Wiley, New York, 1999).
 10. V. A. Markel, *J. Opt. Soc. Am. B* 12, 1783 (1995).
 11. M. Husnik, M. W. Klein, N. Feth, M. König, J. Niegemann, K. Busch, S. Linden, and M. Wegener, *Nat. Photonics* 2, 614 (2008).
 12. K. H. Su, Q. H. Wie, X. Zhang, J. J. Mock, D. R. Smith, and S. Schultz, *Nano Lett.* 3, 1087 (2003); P. Olk, J. Renger, M. T. Wenzel, and L. M. Eng, *Nano Lett.* 8, 1174 (2008); A. M. Funston, C. Novo, T. J. Davis, and P. Mulvaney, *Nano Lett.* 9, 1651 (2009); J. Petschulat, C. Menzel, A. Chipouline, C. Rockstuhl, A. Tünnermann, F. Lederer, and T. Pertsch, *Phys. Rev. A* 78, 043811 (2008); N. A. Gippius, T. Weiss, S. G. Tikhodeev, and H. Giessen, *Opt. Express* 18, 7569 (2010).
 13. A. Taflove and S. C. Hagness, *Computational Electrodynamics: the finite-difference time-domain method*, 2nd ed. (Artech House, Boston, 2000); Y. Zeng and J. V. Moloney, *Opt. Lett.* 34, 1600 (2009).